International Journal of Modern Physics C, Vol. 9, No. 8 (1998) 1247–1261

THERMAL LATTICE-BOLTZMANN MODELS (TLBM) FOR COMPRESSIBLE FLOWS*

GEORGE VAHALA[†,‡,§], PAVOL PAVLO[¶], LINDA VAHALA[‖], and NICOS S. MARTYS[**]

[†]*Department of Physics, William & Mary, Williamsburg, VA 23187*
[‡]*ICASE, NASA-Langley Research Center, Hampton, VA 23681*
[§]*E-mail: vahala@niv.physics.wm.edu*
[¶]*Institute of Plasma Physics, Czech Academy of Sciences, Praha 8, Czech Republic*
[‖]*Dept. of Electrical & Computer Engineering, Old Dominion University Norfolk, VA 23529*
[**]*NIST, Gaithersburg, MD 20899*

Accepted 28 September 1998

The progress and challenges in thermal lattice-Boltzmann modeling are discussed. In particular, momentum and energy closures schemes are contrasted. Higher order symmetric (but no longer space filling) velocity lattices are constructed for both 2D and 3D flows and shown to have superior stability properties to the standard (but lower) symmetry lattices. While this decouples the velocity lattice from the spatial grid, the interpolation required following free-streaming is just 1D. The connection between fixed lattice vectors and temperature-dependent lattice vectors (obtained in the Gauss–Hermite quadrature approach) is discussed. Some (compressible) Rayleigh–Benard simulations on the 2D octagonal lattice are presented for extended BGK collision operators that allow for arbitrary Prandtl numbers.

Keywords: Lattice Symmetries; Linear Stability; Rayleigh–Bernard.

1. Introduction

Lattice-Boltzmann modeling (LBM) of fluids has been under extensive research for over ten years,[1–4] with excellent results reported for incompressible flows. However, the extension of LBM to allow closure at the energy moment level has met with some difficulties. While a kinetic approach to the highly collisional (fluid) regime appears to be inverse statistical mechanics because of the redundancy in phase space information, LBM poses as a discretized molecular dynamics that retains minimal phase space information. The beauty of LBM rests in its ideal parallelization on multiple PE's and its avoidance of the nonlinear Riemann problem which in CFD takes over 30% of the total CPU. In LBM, a kinetic equation is solved for $f(\mathbf{x}, \xi, t)$,

*This paper was presented at the 7th Int. Conf. on the Discrete Simulation of Fluids held at the University of Oxford, 14–18 July 1998.

which in its continuum representation,

$$[\partial_t + \xi \cdot \nabla] f = \Omega(f) \tag{1}$$

in which the collision operator has the simple linear BGK-form (or its extension)

$$\Omega(f) = -\frac{1}{\tau}[f - f^{\text{eq}}]. \tag{2}$$

τ governs the relaxation rate at which f is driven to an f^{eq}. The linear advection, in Eq. (1), can be handled by explicit schemes and here we will utilize a Lagrangian scheme at marginal stability, with CFL = 1. For linear advection, this results in no numerical dissipation or diffusion.

There are several distinct questions that LBM must handle: (a) closure of the kinetic equation, and (b) continuum $\rightarrow$ discrete representation. Here, we follow the standard discretization of LBM (with $f^{\text{eq}} \rightarrow N^{\text{eq}}$) — but now on a nonspacing filling but higher order isotropy velocity lattice. We consider both the 2D octagonal and its 3D extension and examine the linear stability of these higher isotropy lattices. Some results for Rayleigh–Benard convection will be presented (for a 2D octagonal lattice, which allows us to simulate Rayleigh numbers $> 10^8$). Some comments will then be made on the recent discretization using Gauss–Hermite quadratures.

2. Discretization of Velocity Phase Space

On integrating Eqs. (1) and (2) along unperturbed orbits, we have

$$f(\mathbf{x} + \xi\,\delta t,\, t + \delta t) - f(\mathbf{x}, t) = \int_t^{t+\delta t} dt'\, \Omega(t') = -\int_t^{t+\delta t} dt' \frac{f(t') - f^{\text{eq}}(t')}{\tau}. \tag{3}$$

One must now approximate the collision integral in Eq. (3). The standard approximation has been to evaluate this integral just at the lower terminal

$$\int_t^{t+\delta t} dt' \frac{f(t') - f^{\text{eq}}(t')}{\tau} = \frac{f(t) - f^{\text{eq}}(t)}{\tau}\delta t + O(\delta t^2, \ldots) \tag{4}$$

resulting in a 1st-order explicit scheme. A econd-order scheme

$$\int_t^{t+\delta t} dt' \frac{f(t') - f^{\text{eq}}(t')}{\tau} = \frac{1}{2}\left[\frac{f(t+\delta t) - f^{\text{eq}}(t+\delta t)}{\tau} + \frac{f(t) - f^{\text{eq}}(t)}{\tau}\delta t + O(\delta t^3, \ldots)\right] \tag{5}$$

can be readily transformed[5] into an explicit scheme like that generated by Eq. (4), but with the relaxation rate identification

$$\tau_{(5)} \equiv \tau_{(4)} - 0.5 \tag{6}$$

We turn now to the conventional phase velocity ξ-discretization and introduce the notation

$$\begin{array}{lcl} \text{continuum} & \rightarrow & \text{discrete} \\ \xi & \rightarrow & \mathbf{c}_{pi} \\ f(\mathbf{x}, \xi, t) & \rightarrow & N_{pi}(\mathbf{x}, t)\,, \end{array} \tag{7}$$

where the index i, $i = 1, \ldots, b_p$, labels the allowed lattice links at a given speed index p. For a square lattice $b_p = 4$, while $b_p = 6$ for a hexagonal lattice. While these (2D) lattices are space filling, it is important to realize this is not essential. If one chooses a nonspacing filling lattice (e.g., the octagonal lattice[6] in 2D), this will automatically decouple the spatial grid from the velocity lattice. This decoupling has already been encountered in LBM studies that involve nonuniform spatial grids[7] and in finite difference schemes,[8] but these studies were restricted to the standard space-filling velocity lattices.

3. Closure Schemes

On taking moments of the discretized kinetic equation conservation equations one must choose a velocity lattice of sufficient symmetry so as to avoid any discrete lattice symmetry effects from plaguing the final (continuously symmetric) fluid conservation equations. This question of symmetry will also place constraints on the form of the relaxation distribution function N^{eq}.[9] In normalized lattice units, the discretized BGK equation takes the form

$$N_{pi}(\mathbf{x} + \mathbf{c}_{pi}, t + 1) - N_{pi}(\mathbf{x}, t) = -\frac{1}{\tau}[N_{pi}(\mathbf{x}, t) - N^{\text{eq}}_{pi}(\mathbf{x}, t)] \tag{8}$$

with the zero and first moments

$$\rho = \sum_{pi} N_{pi} = \sum_{pi} N^{\text{eq}}_{pi}; \quad \rho\mathbf{u} = \sum_{pi} N_{pi}\mathbf{c}_{pi} = \sum_{pi} N^{\text{eq}}_{pi}\mathbf{c}_{pi}\,. \tag{9}$$

If one wants to impose closure at the momentum level, this is achieved by defining the second moment to be a function of ρ and $\rho\mathbf{u}$ only:

$$\sum_{pi} N_{pi}\, c_{pi\alpha}\, c_{pi\beta} = \sum_{pi} N^{\text{eq}}_{pi}\, c_{pi\alpha}\, c_{pi\beta} = \rho\, c_s^2\, \delta_{\alpha\beta} + \rho\, u_\alpha u_\beta \tag{10}$$

so that the "pressure" $p = \rho\, c_s^2$, where c_s is a sound speed.

On the otherhand, if one wants to close at the energy level, the internal energy e is defined by the 2nd moment (here D is dimensionality of the space)

$$\sum_{pi} N^{\text{eq}}_{pi}\, c_{pi\alpha}\, c_{pi\beta} = \frac{2}{D}\rho\, e\, \delta_{\alpha\beta} + \rho\, u_\alpha u_\beta \tag{11}$$

and then closure is enforced on the 3rd and 4th moments:

$$\sum_{pi} N^{\text{eq}}_{pi}\, c_{pi\alpha}\, c_{pi\beta}\, c_{pi\gamma} = \frac{2}{D}\rho e(u_\alpha\delta_{\beta\gamma} + u_\beta\delta_{\gamma\alpha} + u_\gamma\delta_{\alpha\beta}) + \rho u_\alpha u_\beta u_\gamma \tag{12}$$

$$\sum_{pi} N_{pi}^{\mathrm{eq}}\, c_{pi\alpha}\, c_{pi\beta}\, c_{pi}^2 = \frac{4(D+2)}{D^2}\rho\, e^2\, \delta_{\alpha\beta} + \frac{2}{D}\rho e u^2 \delta_{\alpha\beta} + \frac{2(D+4)}{D}\rho e u_\alpha u_\beta + \rho u_\alpha u_\beta u^2 . \tag{13}$$

The internal energy e is related to the kinetic temperature θ by $e = D\theta/2$. The ideal gas law is $p = \rho\theta$. The moments, Eqs. (11)–(13), are invariant to whether one uses N or N^{eq}.

To exactly satisfy these constraints, Eqs. (9)–(13), one is forced into a polynomial representation for N^{eq}. For energy closure, and to ensure the absence of higher order nonlinearities in the moment equations,[9] N^{eq} is taken in the form

$$N_{pi}^{\mathrm{eq}} = \rho[A_p(e) + B_p(e)\mathbf{c}_{pi}\cdot\mathbf{u} + C_p(e)(\mathbf{c}_{pi}\cdot\mathbf{u})^2 + D_p(e)u^2 + E_p(e)\mathbf{c}_{pi}\cdot\mathbf{u}u^2 + F_p(e)(\mathbf{c}_{pi}\cdot\mathbf{u})^3 + G_p(e)(\mathbf{c}_{pi}\cdot\mathbf{u})^2u^2 + H_p(e)u^4], \tag{14}$$

where the coefficients $A_p(e)\ldots H_p(e)$ are polynomial functions of the internal energy e. The number of different speed lattices, p, that need to be introduced depends critically on the particular chosen velocity lattice.

For closure at the momentum level, the usual form of N^{eq} has $E_p = 0 = \cdots = H_p$, with the internal energy e being simply an external parameter. This standard closure will introduce triple order nonlinearities in the momentum equation — but these spurious terms can be immediately eliminated[9] by allowing E_p and F_p to be nonzero.

It is evident from Eq. (14) that as we proceed from a momentum closure physics to an energy closure physics the only change to LBM is to simply increase the order of expansion $\mathbf{u}$ in the N^{eq}-representation (as well as the number of speed-lattices p). This is a clear indicator why TLBM will be more numerically unstable than LBM.

4. Lattice Symmetries for

The choice of velocity lattice plays a critical role in the numerical stability of TLBM, as is evident from substituting Eq. (14) into Eqs. (9)–(13). In particular we will need to evaluate the nth-lattice velocity moments

$$T^{(n)}_{\alpha\cdots\xi} \equiv \sum_p T^{(n)}_{p,\alpha\cdots\zeta} \equiv \sum_p \sum_i c_{pi\alpha}\cdots c_{pi\zeta} \tag{15}$$

and note there are no spurious nonlinearties introduced into the moment equations if we can ensure $T^{(6)}$-isotropy. For arbitrary regular lattices

$$T^{(4)}_{p,\alpha\beta\gamma\delta} = \psi_p\gamma_{\alpha\beta\gamma\delta} + \phi_p(\delta_{\alpha\beta}\delta_{\gamma\delta} + \mathrm{c.p})$$

$$T^{(6)}_{p,\alpha\beta\gamma\delta\varepsilon\zeta} = \Psi_p\gamma_{\alpha\beta\gamma\delta\varepsilon\zeta} + \Lambda_p(\delta_{\alpha\beta}\gamma_{\gamma\delta\varepsilon\zeta} + \mathrm{c.p}) + \Phi_p(\delta_{\alpha\beta}T^{(4)}_{\gamma\delta\varepsilon\zeta} + \mathrm{c.p}), \tag{16}$$

where $\gamma_{\ldots}$ is the higher rank Kronecker tenssor ($\gamma_{\ldots} = 1$ if all indices are equal, 0 otherwise) and is anisotropic. $\psi_p \cdots \Phi_p$ are lattice geometry-dependent coefficients and "c.p" denotes the cyclic permutation of indices. The 2D lattice vectors are (for integer p)

$$\mathbf{c}_{pi} = p\left(\cos\frac{2\pi[i-1]}{L}, \quad \sin\frac{2\pi[i-1]}{L}\right), \quad \text{where}$$

$$\begin{aligned} &\text{2D square:} && i = 1 \cdots L = 4 \\ &\text{2D hexagonal:} && i = 1 \cdots L = 6 \\ &\text{2D octagonal:} && i = 1 \cdots L = 8 \end{aligned} \tag{17}$$

so that the isotropy properties of $T^{(n)}$ are

2D square: $\psi_p \neq 0 \Rightarrow T_p^{(4)}$ is not isotropic

2D hexagonal: $\psi_p = 0$, but $\Psi_p \neq 0 \Rightarrow T_p^{(4)}$ isotropic, but not $T_p^{(6)}$

2D octagonal: $\psi_p = 0 = \Psi_p = \Lambda_p \Rightarrow T_p^{(6)}$ isotropic.

From this we can immediately conclude that the minimum number of bits of velocity space information required for the specified closure level are:

	2D Square	2D Hexagonal	2D Octagonal
Momentum closure	9 (2-speed)	7 (1-speed)	9 (1-speed)
Energy closure	13 (3-speed)	13 (2-speed)	17 (2-speed)

If one wishes to eliminate the spurious cubic nonlinearities in the conservation equations, then one must use a 17-bit mode TLBM on a 2D square lattice. However, we have found this 17-bit model to be extremely numerically unstable. However the 2D octagonal 17-bit model will automatically guarantee the elimination of this spurious nonlinearity because of the higher order isotropy of this lattice.

4.1. *Lattice symmetries for 3D*

In 3D, there are no such generic isotropic lattices. Typically, one has resorted to the 3D projection of the 4D FCHC.[1] These lattice only have enough symmetry to support $T^{(4)}$-isotropy, a symmetry that is just adequate to recover TLBM (but with the spurious triple order nonlinearities present in the conservation equations).

A canonical basis in D dimensions will consist of a D-dimensional vector with components being permutations of ± 1 or 0. The index "p" now will label the number of nonzero components of that lattice vector grouping, and integer k allows for integer multiples of these base vectors : $\mathbf{c}_{pki} = k\mathbf{c}_{pi}$. A 4D FCHC vector basis consists of the rest particles ($p = 0$) and 3 canonical bases: $p = 2$, $k = 1$ [i.e., 24 vectors formed from the permutations of $(\pm 1, \pm 1, 0, 0)$],; $p = 4$, $k = 1$ [16 vectors

formed from the permutations of $(\pm 1, \pm 1, \pm 1, \pm 1)$] and $p = 1$, $k = 2$ [8 vectors from the permutations of k. $(\pm 1, 0, 0, 0)$]. Since the macroscopic variables $(\rho, \rho \mathbf{u}, e)$ are 3D, the 49-bit 4-vectors must be projected onto 3D space. The 4-vectors with ± 1 component values in the fourth dimension have the same 3D projection (degeneracy 2), so that the resulting TLBM is a 34-bit model

4D : (p, k)	3D Projection (p, k)	Degeneracy	b_p (# bits)
$p = 0$	$p = 0$	1	1
$p = 2, k = 1$	$p = 1, k = 1$	2	6
	$p = 2, k = 1$	1	12
$p = 4, k = 1$	$p = 3, k = 1$	2	8
$p = 1, k = 1$	$p = 0$	2	1
	$p = 1, k = 2$	1	6

This model differs from that constructed directly from 3D composed regular lattices in the appearance of "rest energy particles", i.e., particles possessing energy but not moving in physical space. It is important to note that this 34-bit TLBM rigorously satisfies the constraints Eqs. (9)–(14) — unlike the McNamara *et al.*[10] 3D model or that of He *et al.*[5]

We now proceed to extend the ideas of the 2D octagonal lattice to 3D so that the resulting TLBM model can, for the first time, enforce $T^{(6)}$ isotropy. The 3D extension is nontrivial. We first introduce a scaling factor η_{pk} that will be used in the construction of a new basis set

$$\mathbf{c}^*_{pki} = \eta_{pk} k \mathbf{c}_{pi}\,, \quad i = 1 \cdots b_p \tag{18}$$

so that

$$|\mathbf{c}^*_{pk}|^2 = \mathbf{c}^{*2}_{pk} = pk^2 \eta^2_{pk}\,; \quad \psi_{pk} = k^4 \eta^4_{pk} \psi_p\,; \quad \phi_{pk} = k^4 \eta^4_{pk} \phi_p\,. \tag{19}$$

The requirement that ψ_{pk} vanishes for each group k can now be formally written as

$$\sum_p \psi_{pk} = 0 = \sum_p k^4 \eta^4_{pk} \psi_p\,. \tag{20}$$

In 3D, the lattice constants in Eq. (16) (for $k = 1$)

p	b_p	ψ_p	ϕ_p	Ψ_p	Λ_p	Φ_p
0	1	–	–	–	–	–
1	6	2	0	2	0	0
2	12	−4	4	−52	4	8
3	8	−16	8	128	−16	0

while the leading order coefficients in N^{eq} must satisfy the following constraints:

#1	$\sum_{pk} b_p A_{pk} = 1$		
#2	$\sum_{pk} b_p c_{pk}^2 A_{pk} = 2e$	$\sum_{pk} b_p c_{pk}^2 B_{pk} = D$	
#3	$\sum_{pk} \phi_{pk} A_{pk} = 4e^2/D^2$	$\sum_{pk} \phi_{pk} B_{pk} = 2e/D$	$\sum_{pk} \phi_{pk} C_{pk} = 1/2$
#4	$\sum_{pk} \psi_{pk} A_{pk} = 0$	$\sum_{pk} \psi_{pk} B_{pk} = 0$	$\sum_{pk} \psi_{pk} C_{pk} = 0$
#5			$\sum_{pk} \Phi_{pk} C_{pk} = e/D$
#6			$\sum_{pk} \Psi_{pk} C_{pk} = 0$
#7			$\sum_{pk} \Lambda_{pk} C_{pk} = 0$

where the constraints #5–#7 above ensure the isotropy of $T^{(6)}$.

There are several things to note:

(a) type $p = 1$ particles must always be present in each group k since $\psi_1 > 0$ while $\psi_{2,3} < 0$,
(b) at least 5 different $(p.k)$ — sets are required so that constraints #3–#7 can be satisfied,
(c) at least one $p = 2$ basis must be included, since only $\Phi_2 \neq 0$.

In the following table, we list two possible 3D TLBM models that yield $T^{(6)}$-isotropy:

	p, k	η_{pk}	$\mathbf{c}^*_{pki}$
41-bit model	$p = 1, k = 1$	1	1
	$p = 3, k = 1$	$2^{-3/4}$	1.0299...
	$p = 1, k = 2$	1	2
	$p = 2, k = 2$	$2^{-1/2}$	2
	$p = 3, k = 2$	0.5	1.7321...
53-bit model	$p = 1, k = 1$	1	1
	$p = 2, k = 1$	$2^{-1/2}$	1
	$p = 3, k = 1$	0.5	0.8660...
	$p = 1, k = 2$	1	2
	$p = 2, k = 2$	$2^{-1/2}$	2
	$p = 3, k = 2$	0.5	1.7321...

One of the consequences of enforcing $T^{(6)}$ isotropy in 3D is the decoupling of the velocity lattice from the spatial grid. This will require interpolation following the free-streaming TLBM step in order to evaluate the distribution function at the spatial node site. Because of our free-streaming formulation, the interpolation need only be 1D. It has been verified for the 2D octagonal lattice that the transport coefficients are invariant to second order interpolation.[6]

5. TLBM Linear Stability Analysis[11]

In a linear stability analysis about the unperturbed state

$$\rho(\mathbf{x}) = \rho_0\,, \quad \mathbf{u}(\mathbf{x}) = 0\,, \quad e(\mathbf{x}) = e_0 \tag{21}$$

we linearize N^{eq}

$$N_{p1}^{\mathrm{eq}} = \rho[A_p(e) + B_p(e)\,\mathbf{c}_{pi}\cdot\mathbf{u} + O(u^2)]$$
$$\text{with} \quad A_p(e) = a_{p0} + a_{p1}e + a_{p2}\,e^2\,, \quad B_p(e) = b_{p0} + b_{p1}\,e \tag{22}$$

about the unperturbed distribution function

$$N_{pi}^{\mathrm{unpert}} = A_p^{(0)} = A_p(e_0)\,, \quad \text{for all } \mathbf{x}\,. \tag{23}$$

Note that only the lower order coefficients A_{pk} and B_{pk} in Eq. (14) with $A_{pk} = A_p, B_{pk} = B_p$ (for all p in each group k) appear. Hence one can drop the k-index in what follows.

At $t = 0$ a small perturbation is applied to the distribution function

$$t = 0: \quad N_{pi}^{(0)}(\mathbf{x}) = A_p^{(0)} + \delta N_{pi}^{(0)}(\mathbf{x}) \tag{24}$$

After one lattice-Boltzmann time-step, the perturbed distribution function (after streaming and collisional relaxation)

$$\begin{aligned}\delta N_{pi}^{(1)}(\mathbf{x}) &\equiv N_{pi}^{(1)}(\mathbf{x}) - A_p^{(0)} \\ &= \sum_{q,j}\left[\frac{1}{\tau}\left\{A_p^{(0)} + \left(\frac{\mathbf{c}_q^2}{2} - e_0\right)\frac{dA_p^{(0)}}{de} + (\mathbf{c}_{pi}\cdot\mathbf{c}_{qj})B_p^{(0)}\right\}\right. \\ &\quad \left. + \left(1 - \frac{1}{\tau}\right)\delta_{pq}\delta_{ij}\right]\delta N_{qj}^{(0)}(\mathbf{x} - \mathbf{c}_{qj})\,.\end{aligned} \tag{25}$$

Hence the linear stability of TLBM is determined from the eigenvalues of the (real) iterated map

$$\Xi^{(t+1)} = \mathbf{CS}\,\Xi^{(t)}\,, \tag{26}$$

where $\mathbf{C}$ is the (block diagonal) collisional relaxation matrix, and $\mathbf{S}$ is the streaming matrix (which is nothing but a shift operator). For a 13-bit 2D hexagonal or square lattice on a 512×512 grid, the matrix $[\mathbf{CS}] = 3.41e+06 \times 3.41e+06$, while for the

53-bit 3D model on a $64 \times 64 \times 64$ grid, the matrix $[\mathbf{CS}] = 1.39e+07 \times 1.39e+07 \times 1.39e+07$.

However, an efficient numerical algorithm will take into account that the **C**-matrix consists of J identical $n_s \times n_s \times \cdots$ blocks, where J is the total number of spatial grid points and n_s is the number of velocity bits in the TLBM. The **S**-matrix is used between successive iterations and is simply a shit operation.

The linear stability analysis proceeds via the method of powers to determine the spectral radius ρ_λ. For the 2D hexagonal lattice, an empirical scaling for ρ_λ has been determined[11]

$$\rho_\lambda \approx \left[\frac{1}{L_f}\right], \tag{27}$$

where L_f is the TLBM time iteration at which the distribution function at some grid node becomes negative. Marginal stability corresponds to $L_f \to \infty, \rho_\lambda \to 1+$.

The following stability windows in the internal energy e have been determined for the 4D FCHC projected onto 3D and the 3D "octagonal" TLBM:

Relaxation rate	4D FCHC - 34 bit ($T^{(4)}$-isotropy)	3D "Octagonal" 53-bit ($T^{(6)}$-isotropy)
$\tau = 0.505$	–	$0.28 \le e \le 0.65$
$\tau = 0.55$	$0.67 \le e \le 0.69$	$0.24 \le e \le 0.70$
$\tau = 0.60$	$0.67 \le e \le 0.95$	$0.23 \le e \le 0.70$
$\tau = 0.70$	$0.66 \le e \le 1.06$	$0.09 \le e \le 0.78$
$\tau = 1.00$	$0.60 \le e \le 1.30$	$0.03 \le e \le 0.91$

$\tau \to 0.5+$ corresponds to the viscosity $\mu \to 0$ and Reynolds number $\mathrm{Re} \to \infty$ [see Eq. (30)].

6. Variable Prandtl Number TLBM

If one restricts the TLBM to a single relaxation time τ then the viscosity and the thermal conductivity transport coefficients are necessarily correlated, resulting in a fixed Prandtl number simulation. To model variable Prandtl number flows, one needs only introduce multiple relaxation times into the collision operator[12,13]

$$\Omega_{pi} = -\sum_j X_{ij}[N_{pj} - N_{pj}^{\mathrm{eq}}], \tag{28}$$

where the circulant matrix X_{ij}

$$X_{ij} = \frac{1}{\tau}\delta_{ij} + \frac{\omega}{b_p c_p^2}\mathbf{c}_{pi} \cdot \mathbf{c}_{pj}. \tag{29}$$

The first term in Eq. (29) is the standard BGK collision term, while a second parameter ω is introduced into the second term. Since the matrix **X** is analyti-

cally invertible, one can immediately determine the transport coefficients from a Chapman–Enskog analysis[13]

$$\mu = \rho e\left(\tau - \frac{1}{2}\right); \quad \kappa = 2\rho e\left(\frac{\tau}{1+\omega\tau/2} - \frac{1}{2}\right). \tag{30}$$

However it is a fundamental result of statistical mechanics that μ and κ are density-independent. This can be readily achieved by forcing τ and ω to be functions of ρ. If one introduces parameters $\mu_0(e)$ and $\kappa_0(e)$

$$\tau = \frac{\mu_0(e)}{\rho(\mathbf{x},t)} + \frac{1}{2}; \quad \omega = \frac{4\rho(\mathbf{x},t)}{\kappa_0(e)+\rho(\mathbf{x},t)} - \frac{2}{\tau}, \tag{31}$$

then the final temperature-dependent transport coefficients

$$\mu = \mu_0(e)e, \quad \kappa = \kappa_0(e)e, \tag{32}$$

where μ_0 and κ_0 have the same temperature dependence. The Prandtl number $\mathrm{Pr} = \mu/\kappa = \mu_0/\kappa_0$ is an arbitrary constant. It should also be noted that we can recover any temperature dependence for the transport coefficients. Thus this extended BGK collision operator can readily model the transport coefficients obtained from the detailed nonlinear Boltzmann collision

$$\mu(e) = W_1(\alpha)e^{(\alpha+3)/2(\alpha-1)}; \quad \mathrm{Pr} = \frac{\mu(e)}{\kappa(e)} = \frac{W_1(\alpha)}{W_2(\alpha)} = \text{const.} \tag{33}$$

with the intermolecular force law $\approx r^{-\alpha}$. For hard sphere collisions ($\alpha \to \infty$), $\mu(e) \to e^{1/2}$ while for Maxwell molecules ($\alpha = 5$), $\mu(e) \to e$.

7. Rayleigh–Benard Convection

TLBM can be readily extended to handle the Rayleigh–Benard problem in which there is fluid under gravity between plates separated by a distance H. The lower plate is held at the higher temperature, e_0, while the upper plate temperature is held at a lower temperature: $e_1 < e_0$. The buoyancy versus diffusion effect is handled by the Rayleigh number Ra, which in TLBM is

$$\mathrm{Ra} = \frac{GH^3(e_0 - e_1)\cdot \mathrm{Pr}}{e_{av}^2 \cdot (\tau - 0.5)^2}.$$

McNamara *et al.*[10] had such numerical instability problems in their 3D code that they had to lower the number of constraints, Eqs. (9)–(13), that were to be enforced. In their 2D simulation on a 150×150 hexagonal lattice, numerical instabilities occurred for $\mathrm{Ra} > 3.2e+04$ — even though a Lax Wendroff scheme was introduced with arbitrary time-step.

On our octagonal lattice, however, we have been able to run for $\mathrm{Ra} > 1.0e+08$ on a 128×128 grid and with a temperature range $e_0/e_1 \approx 2.5$. A 3D simulation has been performed on a $121 \times 121 \times 3$ grid using the 34-bit model for $\mathrm{Ra} = 10^5$. In Figs. 1 and 2 we show the results of various Prandtl numbers on Rayleigh–Benard convection at Reynolds number of 1200. For $\mathrm{Ra} = 2 \times 10^5$ and $\mathrm{Pr} = \mu/\kappa = 0.1$

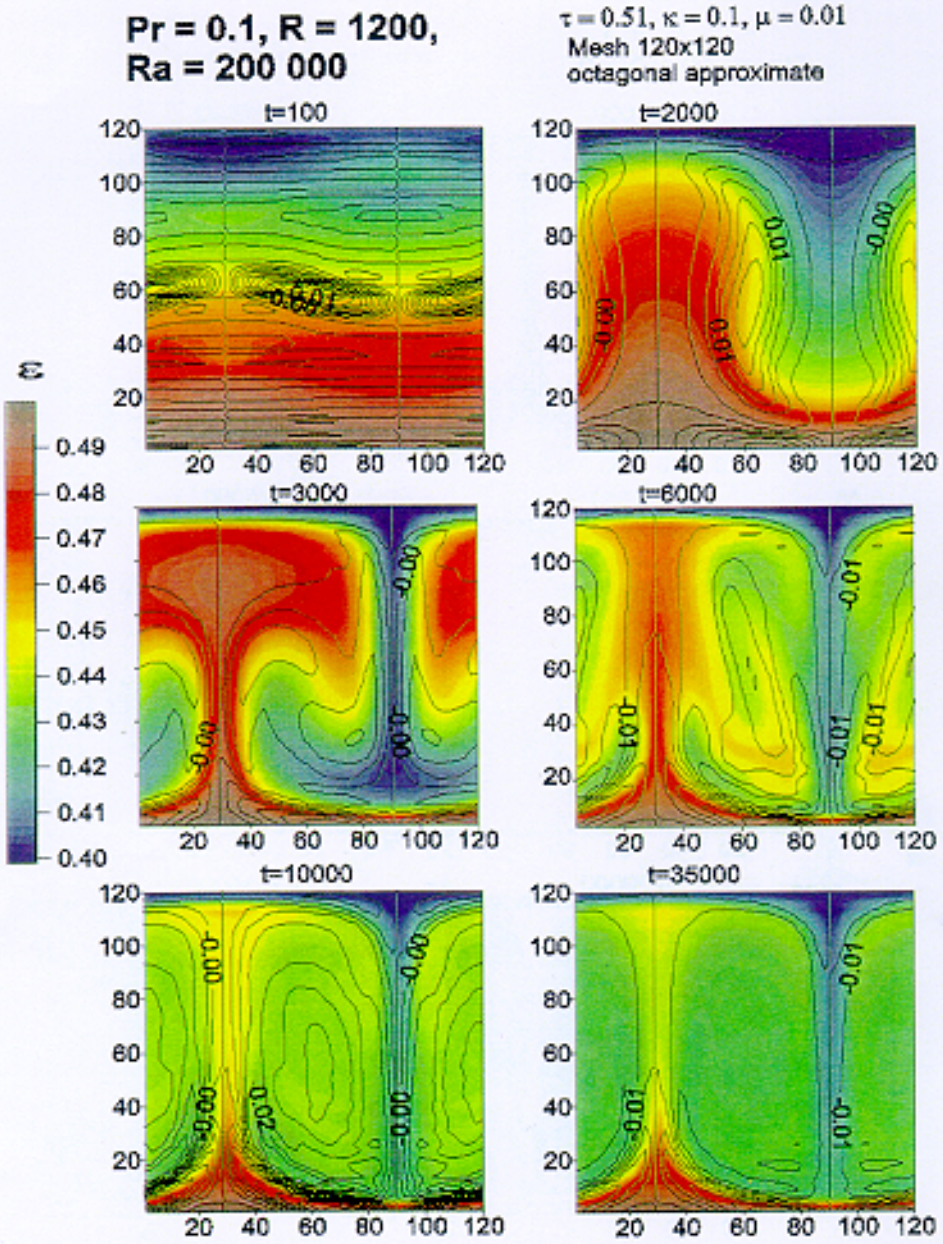

Fig. 1. Rayleigh–Benard convection at Reynolds number 1200 and Ra = 2×10^5. The color surfaces are the internal energy (temperature) while the contour lines are the vorticity. The lower plate ("y = 1") is at temperature 0.5 while the upper plate ("y = 120") is at temperature 0.4. The time-steps are in TLBM time iterations. Note that a quasi-steady state is achieved by 35 K iterations.

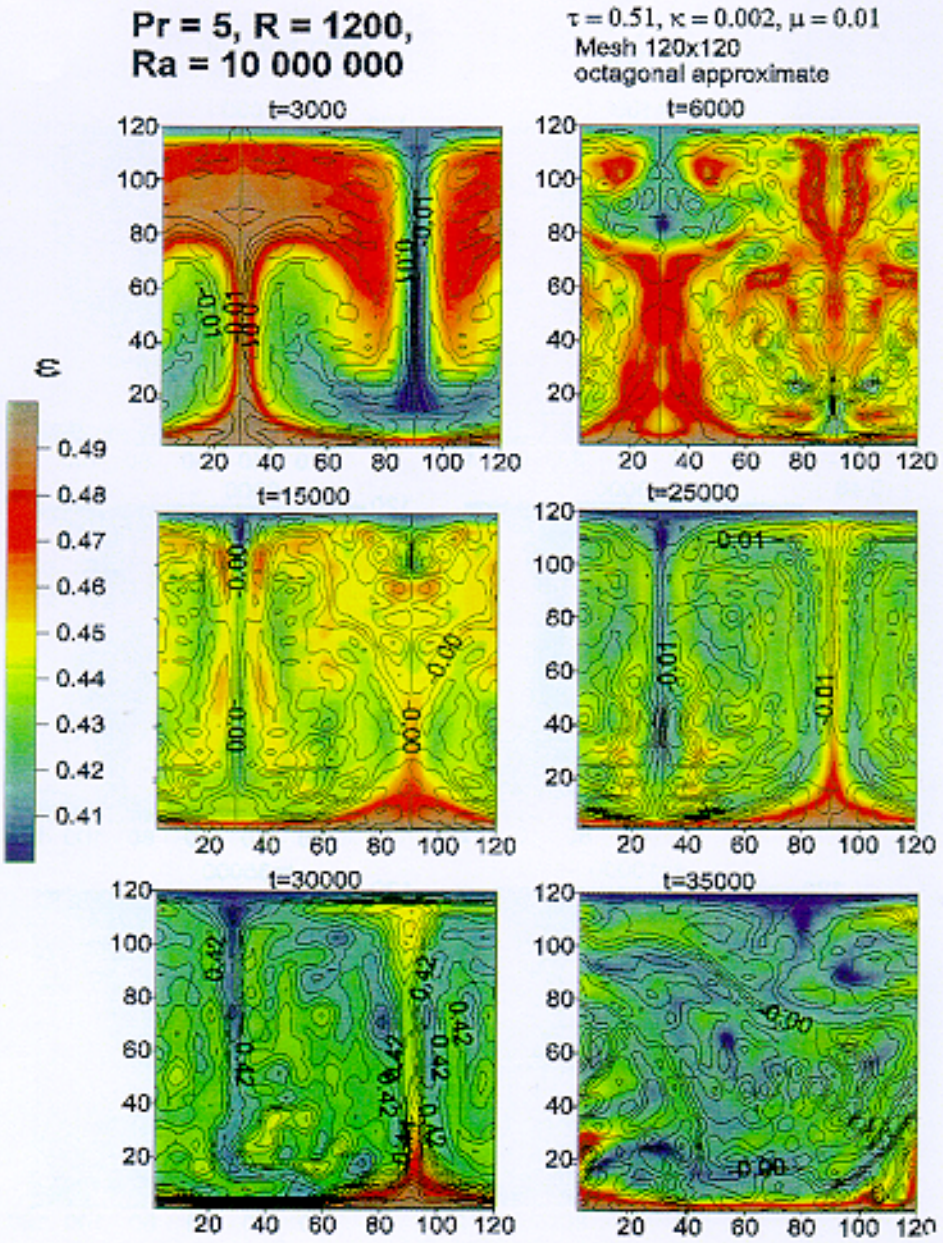

(a)

Fig. 2. The corresponding temperature surfaces and vorticity contours when the conductivity is reduced by a factor of 50 (leading to Ra = 10^7). The flow is no longer laminar and exhibits turbulent bursts. This can be readily seen at 30 K iterations in the vorticity contours for Ra = 2×10^5 (Fig. 1) and Ra = 10^7 (Fig. 2).

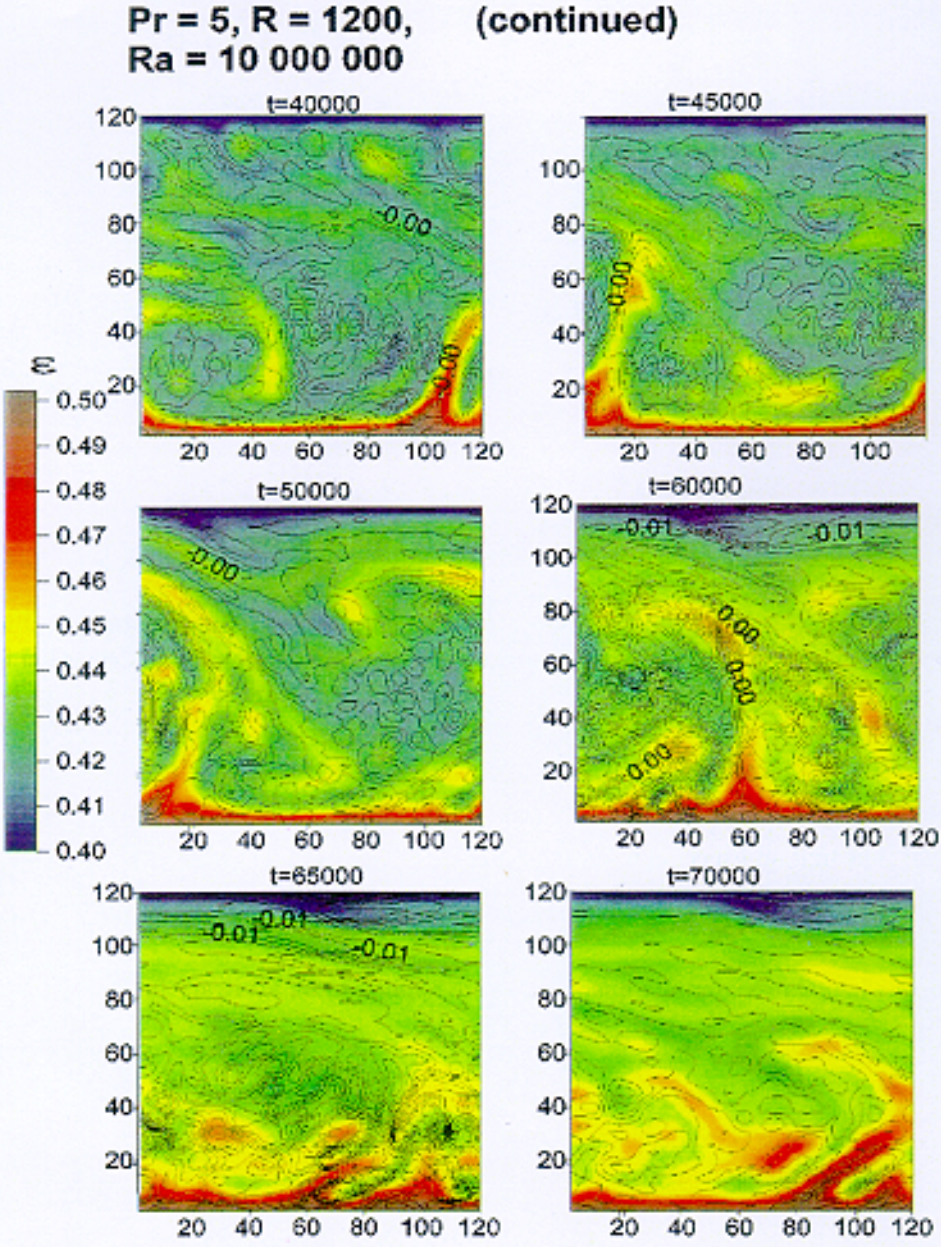

(b)

Fig. 2. (*Continued*)

one sees, Fig. 1, the development of steady-state convection rolls (color plot is the temperature and the contours are the vorticity plots). However, by decreasing the conductivity by a factor of 50 (and thereby increasing the Pr = 5 and Ra = 10^7) one sees the convection rolls giving way to turbulent bursts. It should be mentioned that the typical density variations range from 0.8 to 1.3.

8. Gaussian-Hermite Quadrature Formulation

The Taylor series representation, Eq. (14), has obvious limitations in the achievable Mach number (although with the 2D octagonal grid we can achieve Mach numbers of 0.5). Moreover, this series representation is nonunique (even for a fixed-bit model). An attempt has been made to achieve[14] a unique (for fixed number of bits) representation for N^{eq} in LBM using Gaussian–Hermite quadratures. This approach can be readily applied to TLBM. Consider the continuum representation Eq. (1) and (2), with Maxwellian f^{eq} (in 2D):

$$f^{\mathrm{eq}} = \frac{\rho}{2\pi\theta}\exp\left[-\frac{(\xi-\mathbf{u})^2}{2\theta}\right]$$

$$\approx \frac{\rho}{2\pi\theta}\exp\left[-\frac{\xi^2}{2\theta}\right]\cdot\left\{1+\frac{\xi\cdot\mathbf{u}}{\theta}+\frac{(\xi\cdot\mathbf{u})^2}{2\theta^2}-\frac{\mathbf{u}^2}{2\theta}+\cdots+O(u^5)\right\}, \quad (34)$$

where we have expanded up to fifth order in the mean velocity in order to avoid the spurious third order nonlinearities in the conservation equations. The expansion is needed in order to exactly conserve the moments $\rho, \rho\,\mathbf{u}$, and θ: i.e., one must be able to exactly evaluate (in cartesian coordinates)

$$\int d\xi\, \xi_x^p\, \xi_y^q\, f^{\mathrm{eq}} \quad \text{for} \quad p+q \le 2 \quad (35)$$

and thus find an exact representation for

$$\int_{-\infty}^{\infty} d\zeta\, \zeta^m \exp(-\zeta^2), \quad m \le 6 \quad \text{where} \quad \xi_{x,y} = (2\theta)^{1/2}\zeta\,. \quad (36)$$

Now when Gauss–Hermite quadratures are applied to an arbitrary function $f(\zeta)$

$$\int_{-\infty}^{\infty} d\zeta\, f(\zeta)\exp(-\zeta^2) = \sum_{m=1}^{M} \omega_m\, f(\zeta_m) + O[f^{(2M)}(\zeta_*)]\,, \quad (37)$$

there is an error term dependent on the $2M$th derivative of f. ζ_m are the zeros of the Hermite polynomial H_M and the weights ω_m

$$\omega_m = \frac{2^{M+1}M!\,\pi^{1/2}}{[H_{M+1}(\zeta_m)]^2}\,, \quad \text{with} \quad H_M(\zeta_m) = 0\,. \quad (38)$$

However, for TLBM f is a polynomial — so that for sufficiently large M the quadratures in Eq. (37) are exact. In particular a minimal TLBM is 16-bit with $M = 4$, but this model does not include a rest particle. The 25-bit, $M = 5$ model does have

a rest particle since one of the roots of $H_{2m+1}(\zeta)$ is $\zeta = 0$. In the Guass–Hermite representation, the lattice vectors will always be temperature-dependent, with

$$^{*}\mathbf{c}_{ij} \equiv (\xi_i, \xi_j), \quad \text{with} \quad \xi_0 = 0, \quad \xi_{\pm 1} = \pm 0.96(2\theta)^{1/2}, \quad \xi_{\pm 2} = \pm 2.02(2\theta)^{1/2}. \tag{39}$$

However, the coefficients A_p, $B_p, \ldots$ in the resulting N^{eq} will no longer be functions of q. This is somewhat appealing since the Taylor series in θ of the coefficients clearly indicate somewhat restricted stability bounds on temperature.

It is interesting to note that in the standard polynomial representation, Eq. (14), the lattice vectors are fixed while the coefficients A_p, $B_p \ldots$ are functions of θ. However, if we transform the standard TLBM vectors into lattice vectors with $\theta^{1/2}$-dependence, then the coefficients become independent of θ. While this is very encouraging, it does raise the question of how to accurately handle nonconstant lattice vectors.

References

1. U. Frisch, D. d'Humieres, B. Hasslacher, P. Lallemand, Y. Pomeau, and J.-P. Rivet., *Complex Syst.* **1**, 649 (1987).
2. S. Wolfram, *J. Stat. Phys.* **45**, 471 (1986).
3. R. Benzi, S. Succi, and M. Vergassola, *Phys. Reports* **222**, 145 (1992).
4. S. Chen and G. D. Doolen, *Ann. Rev. Fluid Mech.* **30**, 329 (1998).
5. X. He, S. Chen, and G. D. Doolen, to appear.
6. P. Pavlo, G. Vahala, and L. Vahala, *Phys. Rev. Lett.* **80**, 3960 (1998).
7. X. He, L. Luo, and M. Dembo, *J. Comput. Phys.* **129**, 357 (1996).
8. N. Cao, S. Chen, S. Jin, and D. Martinez, *Phys. Rev. E* **55**, R21 (1997).
9. Y. Chen, H. Ohashi, and M. Akiyama, *Phys. Rev. E* **50**, 2776 (1994).
10. G. R. McNamara, A. L. Garcia, and B. J. Alder, *J. Stat. Phys.* **81**, 395 (1995).
11. P. Pavlo, G. Vahala, L. Vahala, and M. Soe, *J. Comput. Phys.* **139**, 79 (1998).
12. H. Chen, C. Texeria, and K. Molvig, *Int. J. Modern Phys. C* **8**, 675 (1997).
13. M. Soe, G. Vahala, P. Pavlo, L. Vahala, and H. Chen, *Phys. Rev. E* **57**, 4227 (1998).
14. X. He and L. Luo, *Phys. Rev. E* **55**, R6333 (1997).